Relative infaunal bivalve density assessed from split beam echosounder angular information

N. Sánchez-Carnero[a], D. Rodríguez-Pérez[b], N. Zaragozá[c], V. Espinosa[c], J. Freire[d,e]

[a] Grupo de Oceanografía Física, Universidade de Vigo. Campus Lagoas-Marcosende. 36200 Vigo, Spain.

[b] Departamento de Física Matemática y de Fluidos. Facultad de Ciencias, UNED. C/ Paseo de la Senda del Rey, 28040 Madrid, Spain.

[c] Institut d'Investigació per a la Gestió Integrada de Zones Costaneres. C/ Paranimf, 1. 46730 Grau de Gandia, Spain.

[d] Barrabés Next, C. Serrano 16-1, 28001. Madrid

[e] Teamlabs, C. Gobernador 26, 28014. Madrid

Abstract

Management of shellfish resources requires a spatial approach where mapping is a key tool. Acoustic techniques have been rarely used to map infaunal organisms with a patchy distribution. We propose and test the use of split-beam echosounder angular information to assess razor shell presence and relative density. Our statistical approach combines textural analysis standard unsupervised multivariate methods to angular echograms, and dendrograms to identify groups of locations with similar clam densities. Statistical analyses show that the classification is consistent with groundtruthing data and results are insensitive to boat motion or seabed granulometry. The method developed here constitutes a promising tool to assess the relative density of razor clam grounds.

Key words: shellfish beds, stock assessment, split-beam echosounder, angular information, Haralick textural features, benthic habitat mapping

1. Introduction

Several marine invertebrate species have been over-exploited throughout the world and, in some instances, depleted (Jamieson, 1993; Jamieson and Campbell, 1998). During the past 10 years most of the sustainable management strategies aiming to avoid over-exploitation have used spatial regulations such as rotations, marine protected areas (MPA), or territorial use rights. These strategies and their information needs have increased research efforts to develop reliable methods for mapping of species and habitats to both understand and classify marine habitats and manage fishing effort to increase sustainability and/or yield of fisheries (Kostylev *et al.*, 2003; Schimel *et al.*, 2010; Adams *et al.*, 2010).

In the case of benthic species, traditional sampling methods (e.g., *in situ* techniques such as scuba diving, corers, and dredges) used for mapping have limited coverage and a high cost, in terms of time and money. There is a need for a methodology that could provide data of abundance of these benthic species accurately and cost-effectively (Grizzle *et al.*, 2005).

Acoustic methods are the most efficient for mapping and monitoring of large benthic areas (Anderson *et al.*, 2008), and a low-cost alternative to direct sampling for mollusk reefs (Allen *et al.*, 2005; DeAlteris, 1988; Grizzle *et al.*, 2005; Hutin *et al.*, 2005; JiangPing *et al.*, 2009; Lindenbaum *et al.*, 2008; Raineault *et al.*, 2011; Snellen *et al.*, 2008; Wildish *et al.*, 1998). However there is no similar method developed for infaunal mollusk populations, such as razor clams.

Atlantic razor clams inhabit intertidal and subtidal sandy bottoms because oxygen can diffuse unlike in muddy bottoms. These solenids can bury up to 60 cm deep. It has been observed a habitat preference for sandy bottoms with finer granulometry, although this has been related with larval settlement (Holme, 1954; Darriba Couñago and Fernández Tajes, 2011) and thus does not affect their distribution in seeded beds. Furthermore razor clams are not sensitive to sand composition or grain shape, Thus, their presence has to be detected independently of the different acoustic responses caused by the different types of sediments.

The acoustic response from the ocean bottom has two components: the scattering from the rough water-sediment interface, and the volume backscattering. The former is caused by the impedance contrast between sediment and water. The latter originates from sediment grains, shell debris and infaunal species. Both contributions are so mixed that it is difficult to characterize sediment

structure using this information (Anderson *et al.*, 2008; Diaz *et al.*, 2004). It is generally assumed that for high frequency echosounders (i.e. $f \geq 100$ kHz) the backscattered energy mostly originates in the water-sediment interface (because of the high attenuation of the compressional waves in the sediment). However, when shell hash is present in the volume, its scattering may dominate above the critical (grazing) angle for frequencies just above 60 kHz (Lyons, 2005).

The acoustic signal returned to an echosounder not only contains power, but also phase information from the wavefront. Measurement of phase differences at different parts of the transducer allows locating point-like scatterers: the phase difference is related with the angle formed by the scatterer line of sight and the acoustic beam axis. This is actually the principle behind split-beam echosounders (Bodholt *et al.*, 1989; Foote, 1986; Simmonds and MacLennan, 2005). The first commercial split-beam echosounder was introduced in 1984 and it took advantage of new electronic technologies and developments in acoustic signal processing (Foote *et al.*, 1984). The transducer of a split-beam echosounder is usually divided in four quadrants, that allow the measurement of angles in the athwartship and alongship directions. Individual fishes can be tracked and, through continuous insonification, their direction and speed of motion can be assessed (Peirson and Frear, 2003; Boswell *et al.*, 2007; Arrhenius *et al.*, 2000). These angular measurements (or phase differences) also inform about objects protruding from the seabed. Angular information has been applied for acoustic 3D imaging of deep sea-floor (see Cutter and Demer, 2010 and references therein).

Our objective here is to present a method for the discrimination between surface and volume components in the acoustic signal, in order to detect the presence and relative density of razor clams within the seabed. The challenge is to use the angular information provided by a split-beam echosounder in shallow waters to extract the relevant statistical features for discriminating among high density, low density and depleted razor clam beds.

The manuscript is organized as follows. In section 2, the study area, groundtruthing stations and sampling methodology, in the acoustic survey are described. In section 3, the statistical methods used to analyze the split-beam angular information are presented in detail. In section 4, the results obtained with the statistical unsupervised classification are presented. In section 5, these results are discussed regarding their statistical significance and the potential effects that other experimental and environmental factors could have on them. Section 6 presents the main conclusions of the work.

2. Materials and experimental methods

2.1. Study area

The study was carried out in the Ría de Pontevedra (Galicia, NW Spain), an area fished by 10 fishers associations that harvest fish, crustaceans and mollusks (bivalves and cephalopods).

One of the most economically important mollusk in this area is the razor clam, that includes three different species: *Ensis ensis*, *Ensis siliqua* and *Solen marginatus*. All of them are infaunal bivalves with an elongated and semirectangular shape, usually found in high-density patches (beds), surrounded by very low density areas.

The fishers of Ría de Pontevedra harvest 46 different razor clam beds, characterized by continuous sandy areas with an homogeneous mollusk density. These areas are distributed between 0 and 12 m below sea surface, with an average size of 11.76×10^4 m^2 (Fismare, 2011). Three of these razor clam beds, regularly exploited by fishers, were considered for this study: Raxó, Aguete, and A Cova (Figure 1). These three beds are located in sandbars $5-11$ m deep and have approximate areas of 9.3, 6.7 and 28.3×10^4 m^2, respectively. Based on the razor clam harvesting density, the areas were qualitatively described as very productive (Raxó), productive (Aguete), or non productive (A Cova), by local fishers at the time of the survey and we hypothesized that productivity is directly related with density.

2.2. Groundtruthing stations

Six sampling points, two per sandbar (see Figure 3), were set to measure the actual density of razor clams and other (epibenthic) bivalves and the granulometric characteristics of the seabed. Biological communities were characterized using a suction pump with a net retaining individuals of sizes above 1 cm. The number of individuals of razor clams and other bivalves were counted in each sampling station and density was estimated using the area of the sampled frame. Sediment samples were collected with a 30 cm corer. Then they were dried in an oven at 80ºC for two days and apportioned using a 1000 μm analytical sieve (Retsch, Düsseldorf, Germany). Their size distribution was estimated with a laser granulometer (LS200, Beckman Coulter Inc, Brea, CA, USA) and classified according to the Folk classification (Folk, 1954; Jackson and Richardson, 2007). All his information is summarized in table 1.

2.3. Acoustic survey

The acoustic survey was carried out on July 12th, 2009, using a small fishing boat (6.25 m long). A Simrad EK60 scientific echosounder with an ES200-7C split-beam 200 kHz transducer was mounted on a steel pole attached to the hull rail of the boat. The transducer was operated with maximum emitting power (1 kW), minimum pulse length (64 μs), and a sampling rate of 10 pings/s, to obtain the maximum vertical and horizontal resolution. The acoustic survey was made under good weather conditions and keeping the boat speed between 1.5 and 3.5 knots. This speed allows oversampling every bottom point in at least 4 consecutive pings (the split beam angle is 7º and the survey area depth ranges from 5−11 m) ensuring spatial continuity. Positions were recorded into the sounder files using a GPS (Simrad GN33) signal input.

To define the acoustic transects, an imaginary line, parallel to the coast, was defined over each sandbar. Transects were sailed along these lines repeatedly, three times at least each (see Figure 3), switching the course in between, i.e. leaving the coast to the left and right sides; this was later used, to assess differences derived from the ship's course. In total, 14 acoustic transects were recorded: five along the Raxó sandbar, five along Aguete, and four along A Cova, with mean lengths of 550 m, 250 m, and 285 m, respectively.

Angular information from the seabed. The phase distribution of the backscattered signal originates from the bottom surface roughness and the sub-bottom scatterers (razor shells in our study case) within the insonified seabed area.

In previous works split-beam characterization of bottom roughness has been used to discriminate fish aggregations near the seabed (MacLennan *et al.*, 2004) or to improve 3-D bathymetry resolution and seabed classification (Demer *et al.*, 2009; Cutter and Demer, 2010). This technique uses multifrequency transducer assemblies to overcome the baseline decorrelation problem. Our hypothesis is that a similar mechanism in the sub-bottom volume, where impedance fluctuations are due to the presence of benthic biomass, local variations of granulometry, or seabed composition, should give us angular information about the presence of razor clam patches (angle φ in Figure 2a and alongship and athwartship angles in figure 2b).

In the idealized scheme of Figure 2c, the weak scatterers crossing the beam would cause variations

in the echosounder angular information similar to those caused by moving point-like scatterers below the ship. In a naïve representation, as the split-beam passes by a single scatterer, the measured alongship angle will suffer a monotonous variation from positive to negative values, while the athwarth angle detected will show a more uniform value. In the case of a shellfish patch, the multiple scatterings will cause the angles (determined from the phase differences detected) to spread around the actual positions, but the time evolution of the angles will be retained.

However, in the same way their backscattered intensity is superimposed to the rest of the bottom backscatter, making them indistinguishable in the energy echogram, their angular information will compete with the interface returns and sediment volume backscatter drawing a complex picture.

3. Statistical texture analysis of the echogram

Thesplit-beam angular information was processed to provide a textural characterization of the echogram. First order statistics do not offer information about variations in the angular echograms that would denote the presence of razor shells. Thus, a second order statistical procedure, aimed at detecting correlations between nearby acoustic samples, should be applied in the form of textural analysis (Haralick *et al.*, 1973; Zaragozá *et al.*, 2010).

The most used second order statistics is the co-occurrence matrix, whose cell p_{ij} contains the fraction of pairs of the neighboring signal samples (echo bins) having quantized levels *i* and *j*, respectively, in a preset window and after signal quantization in *N* levels (Haralick *et al.*, 1973).

The neighbor samples of a bin can be defined in two natural ways: along the pings (being neighbors the previous and the next bin in the same ping) or along depths (being neighbors the bins of consecutive pings corresponding to the same depth below the detected sea bottom). We will refer to the first neighbor definition as Type 1 (or along pings) and the second one as Type 2 (or across pings). The resulting co-occurrence matrix will be symmetric as if *i* is followed by *j*, then both (*i*, *j*) and (*j*, *i*) bin pairs are counted.

Based on the co-occurrence matrices, Haralick *et al.* (1973) introduced the so called textural features. Thirteen Haralick textural features (denoted as H_1 to H_{13}) have been calculated for both the alongship and athwartship angles. Another textural feature (lacunarity, Lac), describing the relationship between co-occurrence standard deviation and mean value, was also calculated. These

variables are mathematically defined in the Appendix.

We have restricted the textural analysis to those bins comprised between the bottom surface and the equivalent to 30 cm of sediment depth. This depth corresponds to the main insonified region of the echogram and also to the corer sample depth range. Four quantization levels were defined for the angular measures scaled with the mean and standard deviation of the angle value at a given depth below the bottom. If the angle in a bin is φ, then a value $\alpha = (\varphi - \bar{\varphi}) / \sigma_{\varphi}$ is computed, being $\bar{\varphi}$ the mean angle and σ_{φ} its standard deviation in all the bins located at the same depth as the bin considered. Only those angles within two standard deviations around the mean (i.e. $|\alpha| < 2$) have been taken into account in the analyses. These values were quantized to four values corresponding to the four intervals [-2, -1], [-1, 0], [0, 1] and [1, 2].

The procedures for the echogram loading and the computation of the Haralick variables were implemented in the Octave language and are available in the website (http://www. kartenn.es/downloads).

Energy-based acoustic classification. Based on the volume backscatter of the sound wave, a classification of the data could be tested using the roughness and hardness acoustic indexes. These indexes are computed from the first and second acoustic bounces, respectively, and have been introduced as seabed features (Orlowski, 1982). The first echo energy (E1) is computed as the time integral of the received backscattered energy corresponding to the diffuse surface reflection (i.e., without the leading increasing power signal). The second echo energy (E2) is computed as the time integral of the entire second bounce signal. Both energies are normalized by depth applying the correction +20 log(R), where R is the range. This approach using two variables was introduced for seabed classification by Burns *et al.* (1989) and is currently used by the commercial system RoxAnn (Sonavision Limited, Aberdeen, UK).

Multivariate statistical analysis. The multivariate statistical method used was based in Legendre *et al.* (2002) and Morris and Ball (2006) and includes dimensional reduction, principal component analysis (PCA), and clustering analysis of the reduced variables. The original variables included in the analysis were the energy variables (E1, E2) and the alongship and athwartship Haralick variables, corresponding to Type 1 and Type 2 textural features.

The matrix of Haralick textural features was centered and normalized and the PCA was applied (using singular value decomposition whenever more variables than samples were available), to obtain new uncorrelated variables (independent components). Only those components having eigenvalues larger than 1 were kept for the subsequent hierarchical cluster analysis (known as Kaiser's rule). This choice removes noise from the analysis retaining only variables having higher variance than the original (normalized) ones. The clustering analysis of these selected principal component variables was performed using an agglomerative nested hierarchical algorithm to generate dendrograms; complete linkage and Euclidean distances were used. Finally, a stability analysis, based on Jaccard's similarity values (J-values) was used to test the significance of these clusters, i.e., to assess how dependent was the classification obtained of the samples actually used to calculate the dendrogram. Following Henning (2008), when the J-value between two clusters found using different samples is higher than 0.75, then that cluster can be considered a valid stable cluster. The Jaccard similarity value averaged over a number of bootstrap samples will show the expected stability. All these operations were performed using the R open-source statistical software (http://www.r-project.org).

The multivariate statistical analysis has been applied to complete transects and their segments (halves, quarters and eighths of transect) with a bottom-up scale-dependent approach in mind, addressing the spatial distribution of the substrate properties. The vessel orientation with respect to the coast was found to be a relevant factor for the classification; therefore all segment analyses were performed taking only transects or segments leaving the coast to portboard, or taking only those leaving the coast to starboard.

The results obtained from the statistical analysis of the acoustic variables were compared with the groundtruthing data from the stations (depth, sediment granulometry and razor clam and other bivalve abundance) as measured using samples taken by divers. The matching of both data sets (acoustic segments and sampling stations) was performed geographically using GIS software (ArcGis 10.0, ESRI).

4. Results

Here transect and segment classifications are shown based on the acoustical analysis. The sizes of the segments, obtained dividing each transect in equal parts, are variable. For instance, for the largest sandbar (Raxó) where transects were around 500 m in length, the division of a transect in 4

segments provides (in the worst case) segments of about 125 m; for the smaller transects of Aguete, these segments are as small as 40 m. These lengths are representative to study the variations observed along each transect (between groundtruthing points; see figure 3). The most relevant results are presented in figures 3 to 6.

Type 1 features

The hierarchical clustering of all the transects, based on Type 1 textural features, renders a dendrogram with three main clusters; one formed by two Raxó transects and the other two further subdivided in two sub-clusters, one corresponding to Aguete, and the others to Raxó and A Cova, respectively (figure 4). The two Aguete branches correspond to two orientations of the course: one leaving the coast portboard and the other leaving the coast starboard. This suggests that the course is a determinant variable in the classification, and must be factored out to study the effect of the other variables in the classification. For this reason only the analysis of the segments taking into account the course will be presented.

The PCA analysis of segment textural features shows an even distribution of the loadings of Type 1 textural features, denoting high correlation among them. H_1, H_5, H_9, H_{11} and Lac of the along-ship angular signal and H_1, H_3, H_5, Lac of the athwartship angular signal are among the 10 most relevant ones (with higher absolute loadings, weighted by the covariance eigenvalues) for both coast-to-portboard and coast-to-starboard groups of segments.

The hierarchical clustering of the coast-to-portboard segments, shows four main clusters (a1, a2, b1 and b2), each containing segments from only one sandbar (but for a2; see Figure 5a). The geographical distribution of this classification of coast-to-portboard segments can be seen in the thematic map of figure 3. The a1 and a2 (corresponding to Aguete) are statistically stable clusters: their average Jaccard indexes remains above 0.74 after resampling; the other two branches (b1 and b2) are very stable, with J-values above 0.90.

In the case of coast-to-starboard transects, the four main branches of the segment dendrogram, correspond to Raxó (branch a, with two misplaced A Cova segments), other two (b1 and b21) to Aguete, and the last one (branch b22) to A Cova (with one misplaced segment from Raxó; see Figure 5b). With respect to their statistical stability, the Raxó branch, with J-value 0.62, is the less

stable, while all others are more stable with average J-values above 0.73.

Type 2 features

The hierarchical clustering of the transects based on their Type 2 textural features shows four branches: one belonging to Raxó transects, one to A Cova and the remaining two to Aguete (see Figure 4). As for Type 1 features, these results suggest that course may be a determinant variable in the classification and should be factored out prior to studying other variables.

The PCA analysis shows again a balanced distribution of the loadings among the highly correlated Type 1 textural features. H_1, H_2, H_5, H_8, H_9 and Lac of the athwart-ship angular signal and H_8 and Lac of the along-ship angular signal are among the 10 most relevant features in both course-dependent segment classifications.

The hierarchical clustering of the coast-to-portboard segments keeps all of the Raxó segments in one of the four main branches (branch b1 in Figure 6a). Other branches are formed by Aguete segments (a and b22) and A Cova (b21). The average J-values of the A Cova and Aguete (close to station 3) clusters are the lower, but still above 0.71, and only the other Aguete cluster attains a J-value of 0.85 corresponding to a very stable cluster.

The coast-to-starboard dendrogram (Figure 6b), groups Aguete segments in one of the four main branches (a), with Raxó in other branch (b22) and A Cova split between the other two (b1 and b21). The average J-values of the two Aguete clusters (0.90 and 0.95) show them as very stable; the other clusters are also stable, with average J-values above 0.80 (see Table 2).

Energy based classification

The hierarchical clustering of E1 and E2 variables averaged over the transects shows a dendrogram where Raxó transects are grouped in one of the main two branches (figure 7a). However, Aguete and A Cova transects appear mixed in the other one; there is no clear course grouping, as in the case of angular classification. The results based in data resulting from the division of transects in four segments show that Raxó segments remain grouped in one of the two main branches (figure 7b). However, many segments of Aguete and A Cova are also assigned to that branch; thus the transect

classification is not conserved for the segments. In the other main branch, Aguete and A Cova segments are grouped in two sub-branches: one with most of the Aguete segments and the other with a mixed geographical origin.

5. Discussion

All the acoustic transects and segments covering the three sandbars in the study area have been classified using the Type 1 and Type 2 textural features, taking into account the course (leaving the coast to portboard or starboard).

The Aguete bed segments show always two differentiated zones, eastern and western. The other two sandbars, when divided in separate clusters in the dendrograms, do not show this spatial segregation (see thematic map on Figure 2). This is in accordance with the razor clam density of the beds (see Table 1) that shows that Raxó and A Cova have a more even distribution than Aguete. Aditionally the distribution of the segments included in the mixed branches or the distance between neighbor branches cannot be explained by granulometric data or razor shell density alone.

There are no *a priori* reasons for the asymmetry between coast-to-portboard and coast-to-starboard that could lead to a better classification than the one which is obtained when both courses are taken into account. Our conclusion is that probably this difference is caused by the orientation of the transducer (which was always hooked to portboard) with respect to the direction of seabed maximum slope. This relative angle may affect the way the backscattered wave is reflected towards the transducer from the seabottom and the boat hull.

Energy-based classification has been shown to be, at best, unspecific with respect to razor clam density, and our results show that the classification is worse than in the case of the angular information. Furthermore, energy-based classification depends on the scale of analysis because segment classification shows patterns different from transect classification. In this sense the energy-based approach does not discriminate either clam densities or granulometry. For instance, all segments of Raxó, with medium-fine and medium-coarse granulometry, are classified in a separate branch, despite the other two clam beds also have medium-coarse sand in some of their stations. An alternative hypothesis could be that energy-based classification is related with a combination of

both granulometry and total bivalve density; however, no enough samples were available in this study to test it.

4.1. Analysis of the statistical significance of the classification methods

To assess the role of chance in the angular texture classification, the Jaccard mean values have been computed for each cluster in the dendrograms (see Table 2). According to Henning (2008), a J-value of 0.75 can be assumed as a threshold to consider a cluster as stable. Stable clusters are found for all Type 1 coast-to-portboard oriented segment classifications (except for the Aguete station 3 cluster, with a J-value of 0.73); also, the clusters obtained with the Type 2 textures and coast-to-starboard orientation (in fact, all of them are above 0.80) and coast-to-portboard orientation (but for branch b21 of A Cova, with J-value of 0.71). These are the most statistically stable dendrograms.

Another way to assess the statistical stability of the clusters, and thus the significance of the classification, is to test how dependent it is on the acoustic sampling conditions (given by the vessel speed and the ping rate). A numerical experiment, repeating the statistical analysis taking one ping every 2, 4 or 8, was performed. The results of the stability analyses are summarized in table 2. The original labels of the dendrogram were kept, although a part of the branching structure changes (and sometimes is lost), considering the number of segments that a cluster has in common with the original dendrogram. The Type 1 coast-to-portboard and the Type 2 coast-to-starboard dendrograms are the most stable under this resampling. A similar effect is observed when the segments are reduced to one eighth of a transect or less, and the number of segment mixtures increases and the cluster stability decreases. Thus, having a larger number of contiguous pings is crucial to obtain a stable segment classification.

From the point of view of the physical information in the acoustic signal, the Type 1 features should be the less affected by acquisition conditions, such as pitch and roll motions, as they are computed along single pings. Besides, the Type 2 features would capture the variations caused by the advance of the split-beam transducer above the bottom inhomogeneities between consecutive pings.

Type 1 textures distribute segments among their corresponding sandbars including the case when one of these sandbars is first divided into two subclusters (as in the case of Aguete, which is the one with the most heterogeneous razor clam densities). The Type 2 texture classification, requires a larger number of classes to provide a classification distributing the segments among their sandbars,

and also divides one of the homogeneous sandbars (A Cova) in two groups (the coast-to-starboard). Thus, despite being as statistically stable as the Type 1 classification, it does not reflect with the same coherence the groundtruthing characteristics.

The classification groups together segments with similar razor clam densities. However, it is difficult to estimate the minimal density the method could discriminate. For the surveyed razor clam beds, the most robust classifications (according to Jaccard's value criterion) can differentiate between 116 individuals/m^2 and 60 ind/ m^2 in Aguete, and in most cases, between the 124 ind/m^2 in Raxó and the 116 ind/m^2 in Aguete. However, the method includes in the same class the 124 and the 164 ind/m^2 of Raxó (probably because this last station has only two segments close to it). Given the small number of stations, the method sensitivity cannot be statistically assessed.

4.2 Other factors potentially affecting the classification

Energy-based methods, such as those implemented in commercial software as QTC View (Quester Tangent Corporation, Saanichton, Canada), have been found to provide classifications that are insensitive to velocity or pitch and roll motions (Szalay and McConnaughey, 2002). However, the different nature of the angular signal and the co-occurrence statistical analysis suggest the need to take vessel motion into account, for instance, to interpret the similarities between Aguete and Raxó or A Cova.

Thus, boat velocity and pitch and roll motions must be considered as potential nuisance variables in our analysis, i.e., variables potentially affecting the results, although they were not in the focus of our study. The boat velocity was recovered from the recorded GPS position and time. The pitch and roll relative time variations (the echosounder was not equipped with tilt sensors) were inferred from the variations in the acoustic reflectance around near normal insonification (where it is maximum). As the reflection coefficient near normal incidence depends strongly on angle, following a Gaussian law of width proportional to bottom roughness (Lurton, 2002), reflectance variations are expected to amplify the vessel oscillations about the vertical.

With these velocity and tilt relative variations (which, in turn, show a high degree of correlation), the same statistical analysis as for the other variables was applied. The classification results highlight the difference among the Aguete transects and the others; a difference which is not shown in the energy-based classification.

However, these results rule out these nuisance variables as the origin of bivalve clam cartography (in Figure 2). Even if the Aguete transects were different (and this caused their classification in one same branch), Raxó and A Cova would have been properly differentiated by the angular classification; in those cases the effect of the nuisance variables would be negligible for the relative classification.

4.3 Potential use of the methodology.

Despite their economical importance, research efforts devoted to the cartography of infaunal bivalves are scarce. Hence, we will compare our approach with others aimed at the detection and mapping of commercial bivalve species located over the bottom surface (Hutin *et al.*, 2005; Snellen *et al.*, 2008; Kostylev *et al.*, 2003). Those works used different acoustic equipment (singlebeam, and multibeam) and their analyses were based on a classification of the energy response. Hutin *et al.* (2005) groundtruthing rendered a 71% of successful classification of the clam beds and Snellen *et al.* (2008), between 87 and 98%. Our classification results, referred to the segments described in the previous section (spatial resolution better than 125 m), correctly assigned the 93% of the segments to the right clam density class. Kostylev *et al.* (2003) proposed a methodology based in a multibeam echosounder that relates backscatter strength with bivalve clam density. These authors conclude based on a regression analysis that the backscatter could explain 52.4% of variability in the abundance of commercial scallops. The authors suggest the use of this correlation, together with a sediment type stratification, to improve the scallop stock assessment in extended areas. In our case, granulometry in the sampling stations of the three sand bars examined are different enough to rule out a relationship between the angular classification and the granulometry. This, together with the experimental design of transects above the sandbars of interest, is an advantage with respect to a wide area energy mapping that requires taking into account the variability of geophysical features (Kostylev, 2012).

In the present paper, angular information has been shown potentially useful for updating the information about density of infaunal populations of known clam beds. Our method does not yet provide a quantitative relationship between angular features and actual individual density. Contrary to previous methods for mapping bivalve clams (lying above the sea bottom), our approach is focused on clam beds with known positions. In this way, their monitoring is possible with a significantly cheaper acoustic surveying. Moreover, the method is well adapted to evaluate razor

clam patches qualitatively, grouping them in classes of homogeneus relative density.

6. Conclusions

The method introduced in this paper represents a first attempt to use the split-beam echosounder for mapping and monitoring bivalve beds that lay beneath the seafloor (tens of centimeters inside the sediment), as in the case of razor shells. It will be useful to map infaunal bivalve populations (such as the razor clam studied) that form large patches where the density varies smoothly.

We have shown that split-beam angular signal contains relevant information about infaunal bivalve presence and density. The textural features extracted from the angular echogram successfully classified the acoustic transects (or segments of them) according to the abundance of razor clams observed in grountruthing. The unsupervised classification is relative: points with similar razor clam densities are grouped together, although the method does not provide an absolute estimation of razor shell density. To achieve this absolute density estimation further research on the acoustic angular signal received by a split-beam echosounder from the sea bottom would be needed, but it is beyond the objectives of the present work. The method improves the results based on intensity reflection which are not sensitive enough to discriminate volume backscattering. However, it also raises new questions: may clam patches be distinguished from sandy seabed with coarse grain size particles in subsurface? would buried shell hash have similar signatures? would sediment packing (as opposed to mean grain size) have impact on the acoustic scattering? Further research should address these questions.

Appendix A. Haralick textural variables

The textural variables introduced by Haralick *et al.* (1973) are defined in terms of the co-occurrence matrix cell values, p_{ij}. This set of fourteen redundant probability measures quantifies the distance of the co-occurrence matrix from that of a spatially uncorrelated signal. We have retained the order in the original paper: H_1, energy or angular second moment; H_2, contrast; H_3, correlation; H_4, variance; H_5, inverse difference moment; H_6, sum average; H_7, sum variance; H_8, sum entropy; H_9, entropy; H_{10}, difference variance; H_{11}, difference entropy; H_{12}, normalized relative entropy; H_{13}, entropy angle, and H_{16}: maximum correlation coefficient (not used in this paper). Another feature, lacunarity, describes the relationship between co-occurrence standard deviation and mean value of the p_{ij}, whereas all other Haralick variables deal with just one of them at a time. The mathematical expressions used to compute these variables are summarized in Table A.2.

References

Adams C., Harris B., Marino II M., Stokesbury K., 2010, Quantifying sea scallop bed diameter on Georges Bank with geoestatistics, Fisheries Research, 106, 460-467.

Allen Y., Wilson C., Roberts H., Supan J., 2005, High Resolution Mapping and Classification of Oyster Habitats in Nearshore Louisiana Using Sidescan Sonar, Estuaries and Coasts, 28, 435-446.

Anderson J., Van Holliday D., Kloser R., Reid D., Simard Y., 2008, Acoustic seabed classification: current practice and future directions, ICES Journal of Marine Science, 65, 1004-1011.

Bodholt H., Ness H., Solli H., 1989, A new echo-sounder system. In: Proceedings of the Institute of Acoustics, 11 pp. 123-130.

Boswell K., Wilson M., Wilson C., 2007, Hydroacoustics as a Tool for Assessing Fish Biomass and Size Distribution Associated with Discrete Shallow Water Estuarine Habitats in Louisiana, Estuaries and Coasts, 30, 607-617.

Burns, D., Queen, C., Sisk, H., Mullarkey, W., Chivers, R., 1989. Rapad and convenient acoustic sea-bed discrimination for fisheries applications. In: Proceedings of the Institute of Acoustics. Vol. 11. pp. 169-178.

Cutter G., Demer D., 2010, Multifrequency biplanar interferometric imaging. IEEE Geoscience and Remote Sensing Letters, 7, 171-175.

Darriba Couñago S., Fernández Tajes, J., 2011, Systematics and distribution. In: Razor clams: Biology, Aquaculture and Fisheries. Guerra Díaz A., Lodeiros Seijo C., Baptista Gaspar M.and da Costa González F.. Xunta de Galicia, Consellería do Mar, 2011. ISBN:978-84-453-4986-1

DeAlteris J., 1988, The application of hydroacoustics to the mapping of subtidal oyster reefs, Journal of Shellfish Research, 7, 41-45.

Demer D., Cutter G., Renfree J., Butler J., 2009, A statistical-spectral method for echo classification, ICES Journal of Marine Science, 66, 1081-1090.

Diaz R., Solana M., Valente R., 2004, A review of approaches for classifying benthic habitats and evaluating habitat quality, Journal of Environmental Management, 73, 165-181.

MacLennan D.N., Copland P., Amstrong E., Simmonds E., 2004, Experiments on the discrimination of fish and sea bed echoes, ICES Journal of Marine Science, 61, 201-210.

Fismare S.L., 2011, Avaliación da pesquería de navalla (*Ensis arcuatus*) da ría de Pontevedra cara unha explotación sostible: estudio e integración dos aspectos biolóxicos e hidrodinámicos na súa explotación. Tech. rep., Fismare Innovación para la Sostenibilidad S.L., A Coruña, Spain.

Folk R.L. 1954, The distinction between grain size and mineral composition in sedimentary rock nomenclature, Journal of Geology, 62(4), 344-359.

Foote K., 1986, Measurement of fish target strength with a split-beam echo sounder, Jounal of the Acoustic Society of America, 80, 612-621.

Foote K., Kristensen F., Solli H., 1984, Trial of a new split-beam echosounder, Tech. Rep. Document 1984/B: 21, ICES.

Grizzle R., Ward L., Adams J., Dijkstra S., Smith B., 2005, Mapping and characterizing oyster reefs using acoustic techniques, underwater videography and quadrat counts. In: American Fisheries Society Symposium, 41, pp. 152-159.

Haralick R., Shanmugam K., Dinstein I., 1973, Textural features for image classification, IEEE Transactions on systems, man and cybernetics, 3, 610-621.

Hennig C., 2008, Dissolution point and isolation robustness: robustness criteria for general cluster analysis methods, Journal of Multivariate Analysis, 99, 1154-1176.

Holme N. A., 1954, The ecology of British species of Ensis, Journal of the Marine Biological Association of the United Kingdom, 33(1), 145-172.

Hutin E., Simard Y., Archambault P., 2005, Acoustic detection of a scallop bed from a single- beam

echosounder in the St. Lawrence, ICES Journal of Marines Science, 62, 966-983.

Jackson D., Richardson M., 2007, High-frequency seafloor acoustics, Springer, New York.

Jamieson G., 1993, Marine invertebrate conservation: evaluation of fisheries over-exploitation concerns, American Zoology, 33, 551-567.

Jamieson G., Campbell A., 1998, Estimations king crab (paralithodes camtschaticus) abundance from commercial catch and research survey data. In: Proceedings of the North Pacific Symposium on Invertebrate Stock Assessment and Management. NRC Research Press, pp. 73-83.

JiangPing T., Ye Q., XeChang T., JianBo C., 2009, Species identification of Chinese sturgeon using acoustic descriptors and ascertaining their spatial distribution in the spawning ground of Gezhouba Dam, Chinese Science Bulletin, 54, 3972-3980.

Kostylev V., 2012, Benthic habitat mapping from seabed acoustic surveys: do implicit assumptions hold? In: Li, M., Sherwood, C., Hill, P. (Eds.), Sediments, Morphology and Sedimentary Processes on Continental Shelves: Advances in technologies, research and applications. Wiley-Blackwell, Chichester, England

Kostylev V.E., Courtney R.C., Robert G.., Todd B.J., 2003, Stock evaluation of giant scallop (*Placopecten magellanicus*) using high-resolution acoustics for seabed mapping, Fisheries Research, 60, 479-492.

Legendre P., Ellingsen K., Bjørnbom E., Casgrain P., 2002, Acoustic seabed classification: improved statistical method, Canadian Journal of Fisheries and Aquatic Sciences, 59, 1085-1089.

Lindenbaum C., Bennell J., Rees E., McClean D., Cook W., Wheeler A., Sanderson W., 2008, Small-scale variation within a Modiolus modiolus (Mollusca: Bivalvia) reef in the Irish Sea: I. Seabed mapping and reef morphology, Journal of Marine Biology Association of the United Kingdom, 88, 133-141.

Lurton X., 2002, An Introduction to Underwater Acoustics. Principles and Applications, Springer-Verlag, New York.

Lyons P., 2005, The potential impact of shell fragment distributions on high-frequency seafloor backscatter, IEEE Journal of Oceanic Engineering, 30, 843-851.

Morris L., Ball D., 2006, Habitat suitability modeling of economically important fish species with commercial fisheries data, ICES Journal of Marine Science, 63, 1590-1603.

Orlowski A., 1982, Application of multiple echoes energy measurements for evaluation of sea bottom type, Oceanologia 19, 61-78.

Peirson G., Frear P., 2003, Fixed location hydroacoustic monitoring of fish populations in the tidal River Hull, north-east England, in relation to water quality, Fisheries Management and Ecology, 10, 1-12.

Raineault N., Trembanis A., Miller D., 2011, Mapping Benthic Habitats in Delaware Bay and the Coastal Atlantic: Acoustic Techniques Provide Greater Coverage and High Resolution in Complex, Shallow-Water Environments, Estuaries and Coasts, 35(2), 682-699.

Rodríguez-Pérez D., Sánchez-Carnero N., Freire J., 2013, A pulse-length correction to improve energy-based seabed classification in coastal areas, (submitted)

Schimel A., Healy T., Johnson D., Immenga D., 2010, Quantitative experimental comparison of single-beam, sidescan, and multibeam benthic habitat maps, ICES Journal of Marine Science, 67, 1766-1779.

Simmonds E., MacLennan D., 2005, Fisheries acoustics, 2nd Edition. Blackwell Publishing, Oxford.

Wildish D., Fader G., Lawton P., MacDonals A., 1998, The acoustic detection and characteristics of sublittoral bivalve reefs in the Bay of Fundy, Continental Shelf Research, 18, 105-113.

Zaragozá N., Sánchez-Carnero N., Espinosa V., Freire J., 2010, Acoustic techniques for solenoid bivalve mapping. In: Proceedings of the European Conference on Underwater Acoustics, Vol. 1, pp. 139-144.

Table 1: Groundtruthing data and harvesting information provided by the local fishers for the three razor clam beds. The last four columns show the clusters in figures 5 and 6 with their elements (transect segments) geographically closer to these stations; stars denote those clusters with mixed segments.

Bank	Station	Depth (m)	Sand granulometry (Folk classification)	Razor density (indiv./m2)	Other infaunal bivalves (indiv./m2)	Type 1 Portboard	Type 1 Starboard	Type 2 Portboard	Type 2 Starboard
Raxó	1	5.4	Medium-fine	High (124)	112	b2	a*	b1	b2_2
	2	6.4	Medium-coarse	High (164)	16	b2	a*	b1	b2_2
Aguete	3	11	Medium-fine	Low (60)	16	a1	b1	a	a2
	4	7.2	Medium-coarse	Medium (116)	52	a2*	b2_1	b3*	a1
A Cova	5	10.6	Coarse	None (0)	8	b1	b2_2	b2	b1
	6	11.4	Medium-coarse	None (0)	52	b1	b2_2	b2	b2_1

Table 2: Average Jaccard indexes (measuring cluster statistical stability), estimated through bootstrap, of the classification clusters under different subsampling ratios: 1/1 (using all the pings), 1/2 (one every two pings), 1/4 and 1/8. Branch notation is the same as in Table 1 and Figures 5 and 6.

Type 1

Portboard clusters	Jaccard average				Starboard clusters	Jaccard average			
	1/1	1/2	1/4	1/8		1/1	1/2	1/4	1/8
a1	**0,74**	0,73	0,88	(lost)	**a**	**0,62**	0,85	0,64	(lost)
a2	**0,79**	0,77	0,88		**b1**	**0,73**	0,52	0,52	
b1	**0,98**	0,96	0,87		**b21**	**0,84**	0,72	0,52	
b2	**0,92**	0,78	0,99		**b22**	**0,81**	0,90	0,59	

Type 2

Portboard clusters	Jaccard average				Starboard clusters	Jaccard average			
	1/1	1/2	1/4	1/8		1/1	1/2	1/4	1/8
a	**0,85**	0,82	(lost)	(lost)	**a1**	**0,95**	0,91	0,88	0,64
b1	**0,82**	0,87			**a2**	**0,90**	0,87	0,91	0,77
b21	**0,71**	0,62			**b1**	**0,81**	0,67	0,79	0,82
b22	**0,75**	0,74			**b21**	**0,82**	0,81	0,68	0,76
					b22	**0,80**	0,78	0,76	0,76

Table A.3: Mathematical definitions of the Haralick textural variables.

Energy or Angular second moment:	$H_1 = \sum_{ij} p_{ij}^2$	Sum entropy	$H_8 = \sum_k p_k^+ \log \frac{1}{p_k^+}$
Contrast	$H_2 = \sum_k k^2 p_k^-$	Entropy	$H_9 = \sum_{ij} p_{ij} \log \frac{1}{p_{ij}}$
Correlation	$H_3 = \frac{1}{s^2} \sum_{ij} (i-m)(j-m) p_{ij}$	Differences variance	$H_{10} = \sum_k (k-n^-)^2 p_k^-$
Variance	$H_4 = s^2 = \sum_i (i-m)^2 p_{i\times} = \sum_j (j-m)^2 p_{\times j}$	Differences entropy	$H_{11} = \sum_k p_k^- \log \frac{1}{p_k^-}$
Inverse mean distance	$H_5 = \sum_{ij} \frac{p_{ij}}{1+(i-j)^2}$	Relative normalized entropy	$H_{12} = \frac{\sum_{ij} p_{ij} \log \frac{1}{p_{ij}} - \sum_{ij} p_{ij} \log \frac{1}{p_{i\times} p_{\times j}}}{\max\left\{ \sum_i p_{i\times} \log \frac{1}{p_{i\times}}, \sum_i p_{\times j} \log \frac{1}{p_{\times j}} \right\}}$
Sum average	$H_6 = n^+ = \sum_k k p_k^+$	Entropic angular measure	$H_{13} = \sqrt{1 - \exp\left[-2 \sum_{ij} p_{i\times} p_{\times j} \log \frac{1}{p_{i\times} p_{\times j}} \right]}$
Sum variance	$H_7 = \sum_k (k-n^+)^2 p_k^+$	Lacunarity	$Lac = \sqrt{N \sum_{ij} p_{ij}^2 - 1}$
Auxiliary definitions			
$p_k^+ = \sum_{\lvert i+j \rvert = k} p_{ij}$	$p_k^- = \sum_{\lvert i-j \rvert = k} p_{ij}$	$p_{i\times} = \sum_j p_{ij}$	$p_{\times j} = \sum_i p_{ij}$	$n^- = \sum_k k p_k^-$

Figure 1: Study area in the Ría de Pontevedra; highlighted are the clam beds under study.

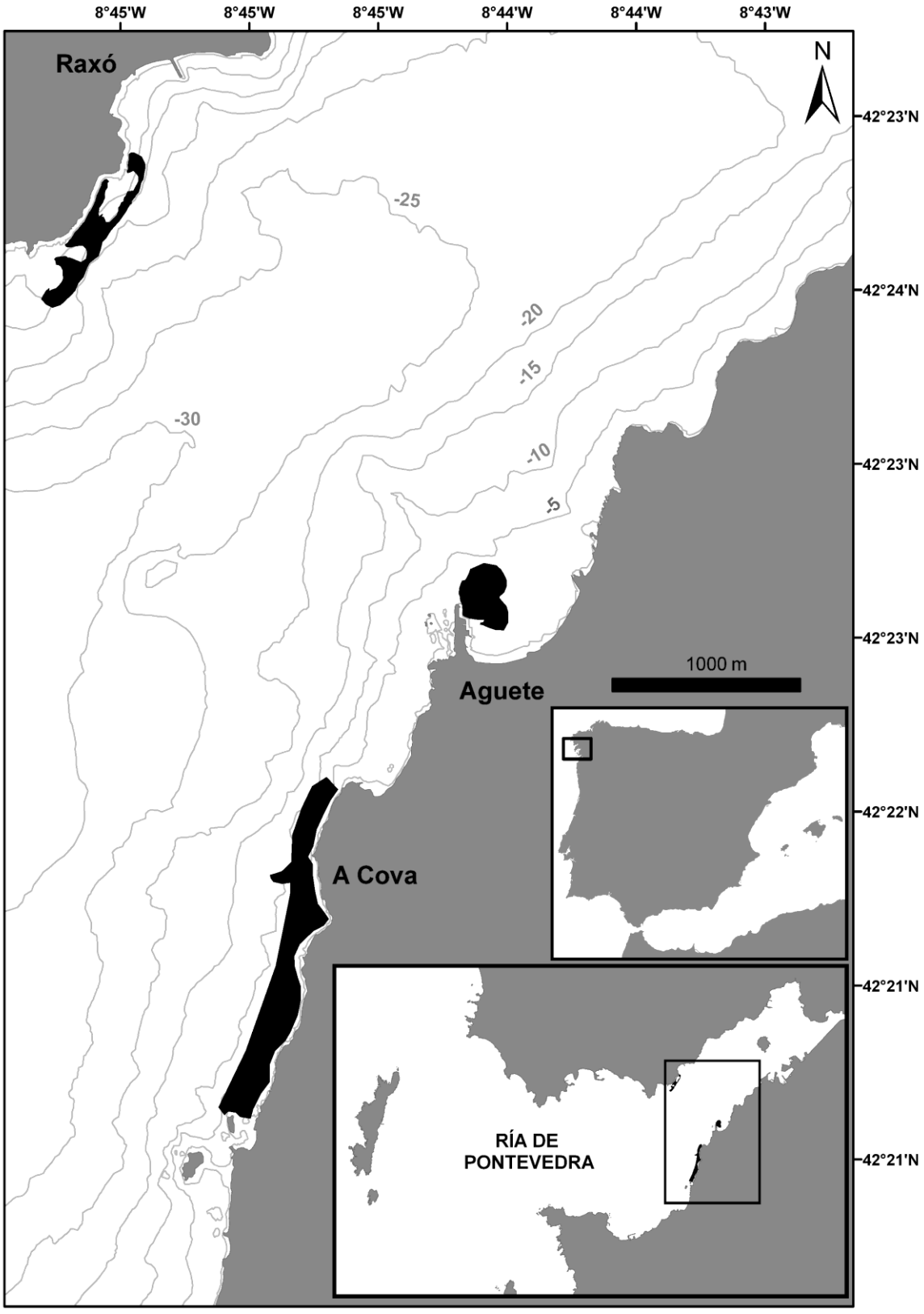

Figure 2: Geometry of the acquisition (a) and angles scheme (b) of the split-beam angular assignation for the case of buried scatterers in a sedimentary bottom. Also the expected temporal evolution of the measured angles as the transducer advances is depicted (c).

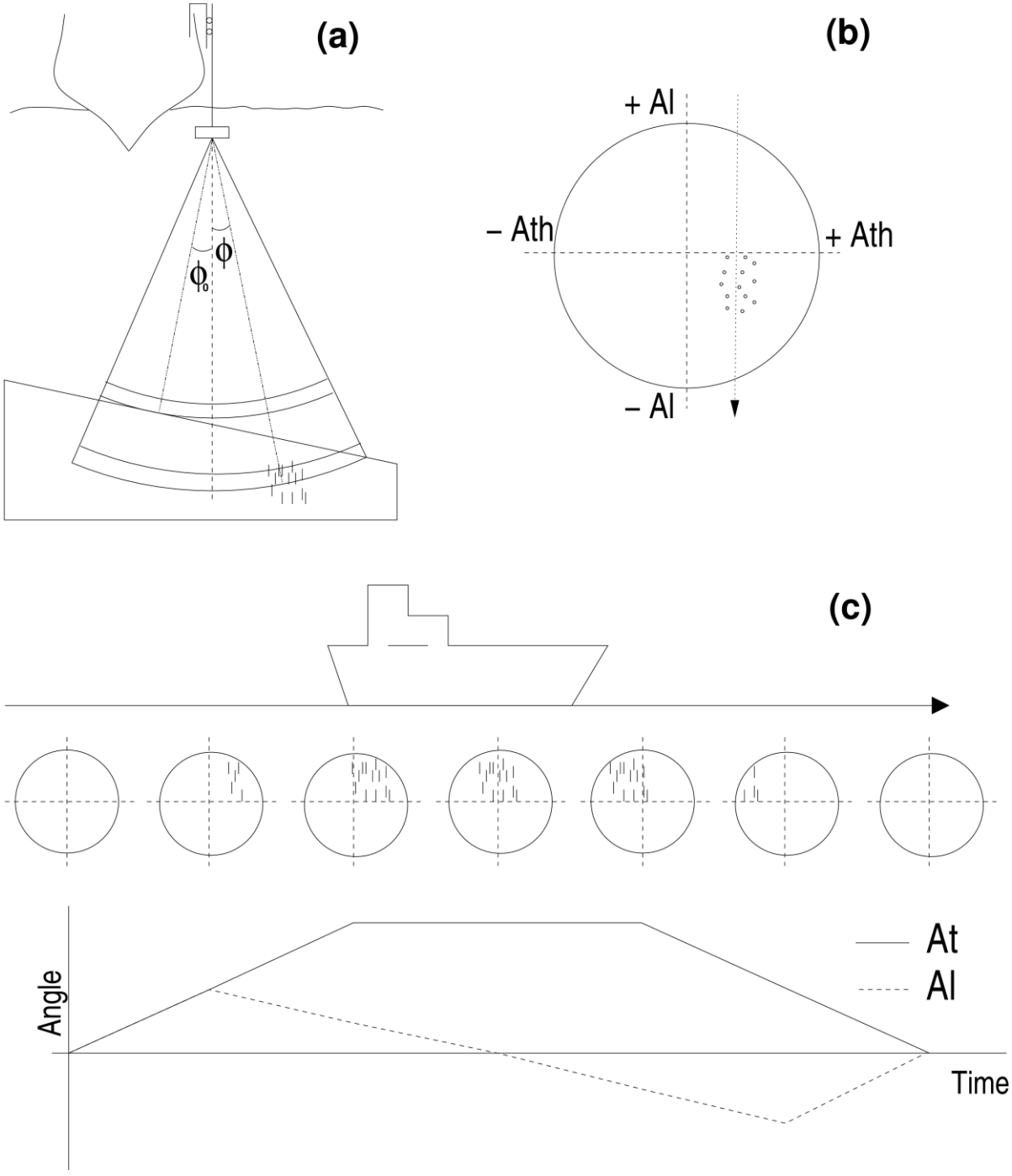

Figure 3: Acoustic transects over the the Raxó (left), Aguete (lower right) and A Cova (upper right) beds. The colors correspond to the dendrogram branches shown in Figure 5 (Type 1 coast-to-portboard dendrogram). A graphical summary for each groundtruthing station in included (according to information in Table 1).

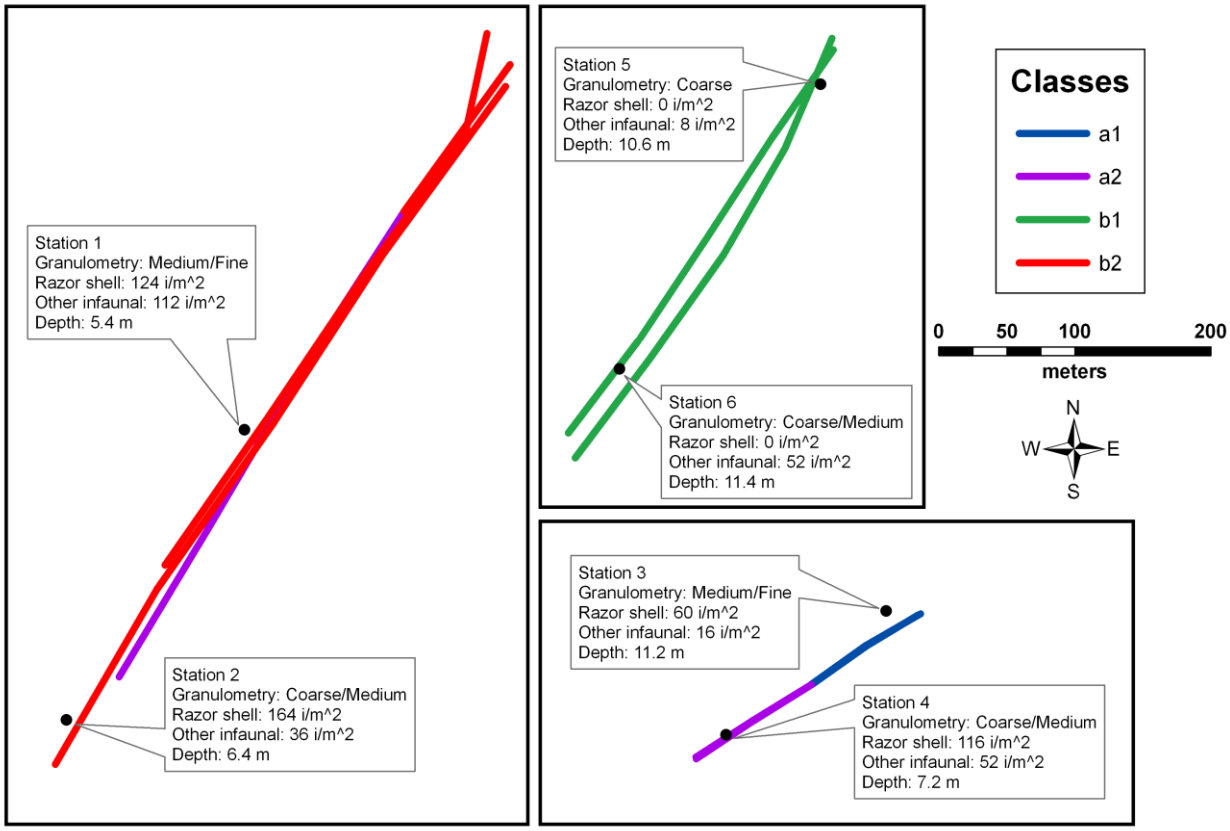

Figure 4: Dendrogram and classification of transects based on Type 1 (upper) and Type 2 (lower) features. Every leaf of the tree is labeled with the initial of the sandbar (according to table 1) enclosed in a circle or a square, denoting that corresponding transect was sailed leaving the coast to portboard or starboard, respectively.

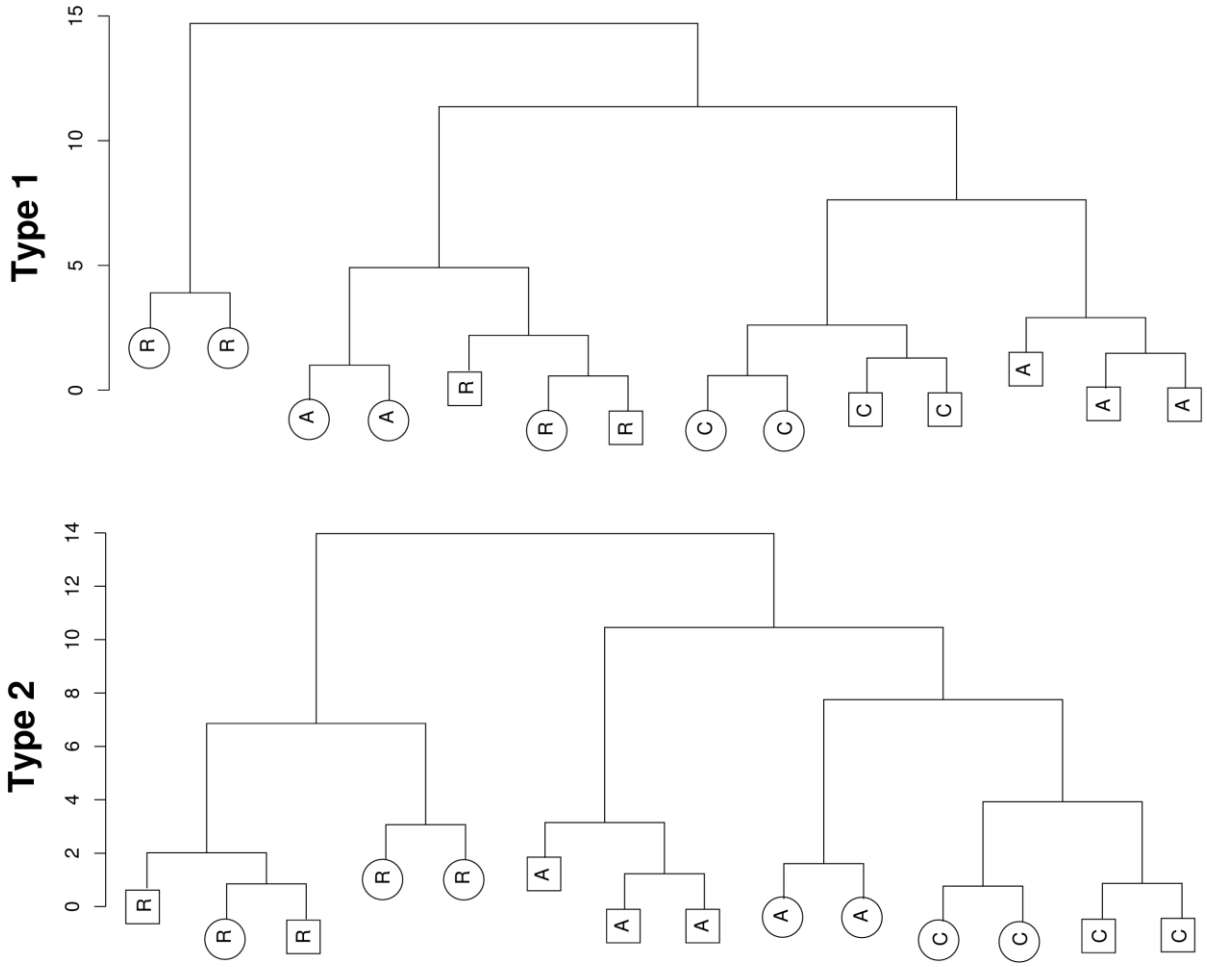

Figure 5: Dendrogram and classification of the segments based on Type 1 features with courses divided in (a) coast-to-portboard and (b) coast-to-starboard. Every leaf of the tree is labeled with the initial of the sandbar and the number of its nearest groundtruthing point (according to table 1). The lower-case letters followed by numbers denote branches and sub-branches of the dendrogram.

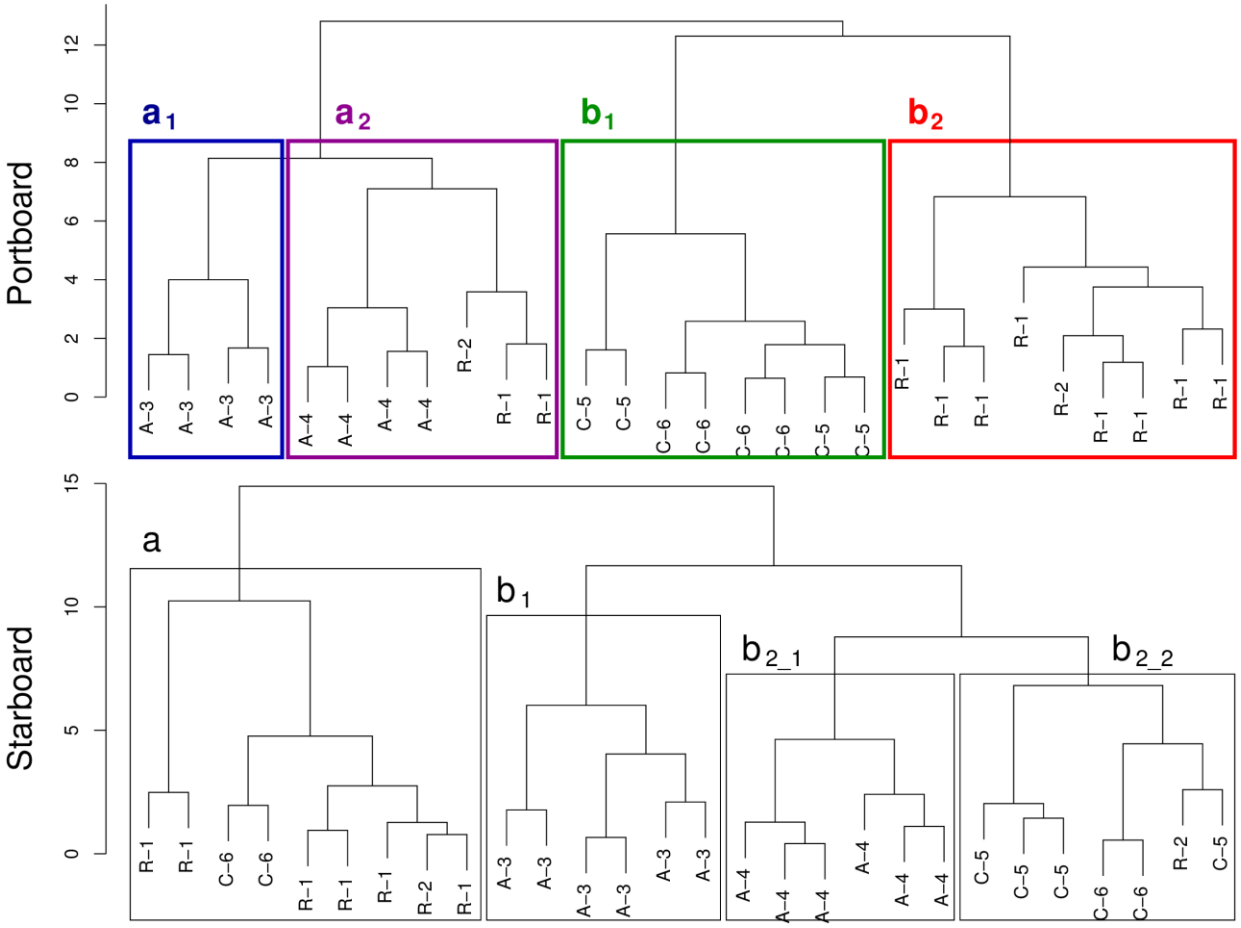

Figure 6: Dendrogram and classification of the segments based on Type 2 features with courses divided in (a) coast-to-portboard and (b) coast-to-starboard. Every leaf of the tree is labeled with the initial of the sandbar and the number of its nearest groundtruthing point (according to table 1). The lower-case letters followed by numbers denote branches and sub-branches of the dendrogram.

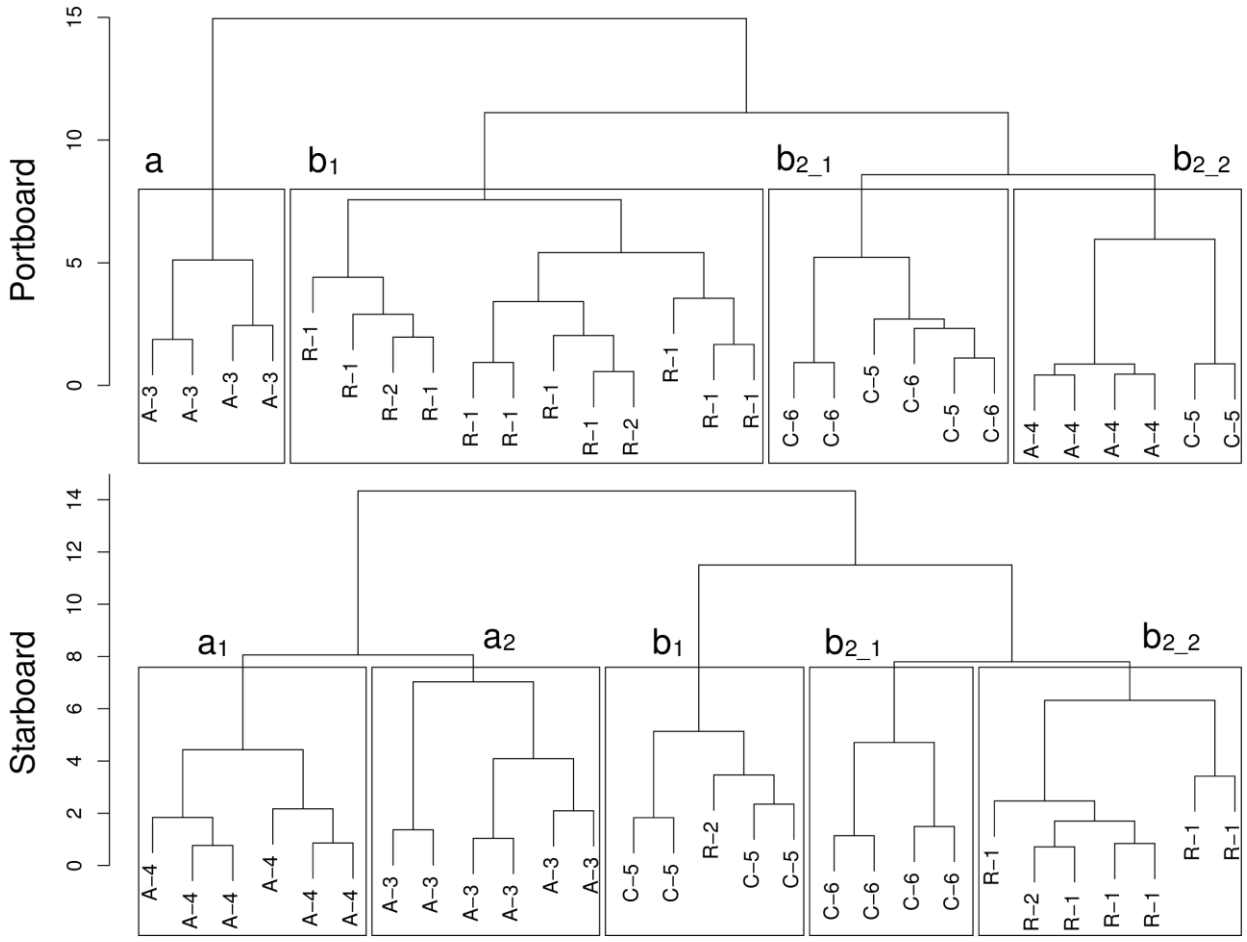

Figure 7: Dendrogram and classification of transects (a) and segments (b) based on energy features E1 and E2.